Enhancement characteristics of laser-induced plasma confined by hemispherical cavities in different materials

Xiaolong Li[1] · Jingge Wang[1] · Hehe Li[1] · Xinzhong Li[1] · Miaomiao Tang[1] · Liping Zhang[1] · Qi Wang[2,3]

Abstract

A hemispherical cavity can be used to improve the sensitivity of laser-induced breakdown spectroscopy by increasing the emission spectra of the plasma. In this work, laser-induced plasma plume images were obtained with and without confinement. The results have confirmed that the reason for the signal enhancement caused by the hemispherical cavity was the reflected shockwave "compressing" effect. The dependence of spectral signal enhancement on the material property of the cavities was investigated. Four cavities in different materials, which include K-resin, aluminum alloy, photosensitive resin and nylon, were used to confine the plasma. It has shown that the material physical properties of the cavities influence the enhancement effect. We found that the main influencing factor was surface roughness of the material. Smoother cavity surfaces induced stronger enhancement effects due to the larger specular reflection component of the reflected shockwave and the more intense subsequent interaction between the plasma and shockwave. The spectral intensities of the characteristic lines approximately doubled with surface roughness values changing from 0.2 to 16.1.

1 Introduction

The rapid development of laser technology [1, 2] has recommended the use of laser-induced breakdown spectroscopy (LIBS) [3, 4] as a powerful method of analyzing the elemental composition of materials. The significant advantages associated with LIBS, which include the absence of the need for sample preparation, nearly nondestructive testing procedures, rapid real-time analysis, and multi-elemental analysis, have led to its wide application in many fields such as industrial process monitoring [5, 6], food safety [7], and space exploration [8, 9], among others.

However, there are several drawbacks associated with the technology, including low detection sensitivity in comparison with other analytical techniques, which limits its development and narrows its application. To improve its sensitivity, many methods, such as magnetic confinement [10, 11], dual-pulse excitation [12, 13], spark discharge [14], and spatial confinement [15, 16], have been proposed. Among these methods, spatial confinement has attracted the interest of most researchers because of its high efficiency and simple implementation compared with other enhancement methods. Gao et al. [17] used two parallel Al plates at distances of 8, 10, 12, and 14 mm to confine the plasma generated by a nanosecond YAG laser, and the corresponding maximum enhancement factors were approximately 2.4, 3.9, 3.8, and 2, respectively. Wang et al. [18] used a moderate cylindrical cavity to improve the precision of LIBS. It was reported in that study that the confinement configuration could both reduce the shot-to-shot fluctuation and increase the signal repeatability [19]. To clarify the mechanism of plasma enhancement using a cylindrical cavity, Li et al. [20] measured the spatially and temporally resolved spectra both with and without the cylindrical cavities. It was found that the spectral emission intensities of plasma generated using cylindrical cavities were enhanced after several microseconds and that the enhanced emission regions moved to higher locations above the sample over time. Fu et al. [15] obtained the plasma plume images and shockwave images for both the flat surface case and the rectangular cavity case. It was reported that the enhancement effect could be explained as a reflected shockwave "compression" effect. It

✉ Jingge Wang
   wangjingge1987@126.com

1   School of Physics and Engineering, Henan University of Science and Technology, Luoyang 471023, China

2   Key Laboratory of High Magnetic Field and Ion Beam Physical Biology, Institute of Technical Biology and Agriculture Engineering, Hefei 230031, China

3   Hefei Institutes of Physical Science, Chinese Academy of Sciences, Hefei 230031, China

was also verified that the spectral enhancement effect was related to the properties of the confinement units. Su et al. [21] optimized the sizes of cylindrical cavities to obtain the best signal quality. The parallel plate and the cylindrical cavity can only compress the plasma plume in one and two dimensions, respectively. Guo et al. [22] first proposed the method of hemispherical cavity confinement to enhance plasma optical emissions in three dimensions and a significant spectral enhancement (factor > 12) in the emission of low-concentration Mn atomic lines was also observed. In our previous study [23], the size of the hemispherical cavity was optimized and the temporal and spatial evolution of the spectra from the plasma was compared while confined and unconfined by the hemispherical cavity. It was demonstrated that the optimal diameter of the cavity was 10 mm and that the plasma was compressed in three dimensions by the hemispherical cavity confinement. Up to now, it is found that the research on spectral enhancement focuses mainly on optimizing the shape and size of the constrained layer. However, Zhou et al. [24] have investigated the relationship between the rigidity of confining medium and laser-induced shockwave. It was demonstrated that an appropriate overlay rigidity can increase peak pressure of laser-induced shockwave more effectively than flexible overlay. Hong et al. [25] studied the characteristics of a laser-induced shockwave under different confining conditions. They have pointed that the confining material has a great effect on the laser-induced plasma-generating process. Peyre et al. [26] have also indicated that the laser shockwave is closely related to the surface properties of the constraining layer. It should be noted that the change of the characteristics of the shockwave will cause the differences in the interaction between the shockwave and the laser-induced plasma, which in turn affect the spectral signal. Therefore, it is necessary to study the influence of the constrained layer material on

the laser-induced plasma. In the present study, hemispherical cavities constructed of different materials were used to confine the plasma generated from a steel alloy sample. The effect of the material properties of the cavity on plasma enhancement was studied.

2 Experimental setup

A schematic diagram of experimental setup for the spatially confined LIBS is shown in Fig. 1. A 1064 nm Q-switched Nd:YAG laser with pulse duration of 8 ns was used to generate the plasma. The laser beam with pulse energy of 150 mJ was focused through a hole (diameter, 3 mm) on the top of the hemispherical cavity (diameter, 10 mm) onto the steel alloy target surface using a plano-concave lens with a 100 mm focal length. The cavities constructed of different materials were placed tightly onto the surface of the sample. The plasma emission generated inside the cavity was focused into an optical fiber using a lens with a 100 mm focal length through a straight slot (height 2.5 mm, radius 1.5 mm) on one side of the hemispherical cavity. The core diameter of the optical fiber was 0.1 mm. The plasma emission was sent for analysis to an Echelle spectrometer (Andor technology, Mechelle 5000) equipped with an intensified charge-coupled device (ICCD) detector (Andor technology, iStar DH-334). The ensemble provided a spectral resolution in the spectral range from 230 to 920 nm and a resolution power ($\lambda/\Delta\lambda$) of 5000. A delay generator (SRS, DG645) controlled the time delay between the laser and ICCD. The ICCD detector was operated in the gated mode. The gate delay and width of the ICCD were adjusted so that spectra could be obtained at different time delays after the laser pulse.

The repetition frequency of the laser was set to 1 Hz. For each new measurement, before spectral collection, 20

Fig. 1 Schematic diagram of the experimental setup. (Illustration: the materials from left to right are K-resin, aluminum alloy, photocurable resin, and nylon, respectively)
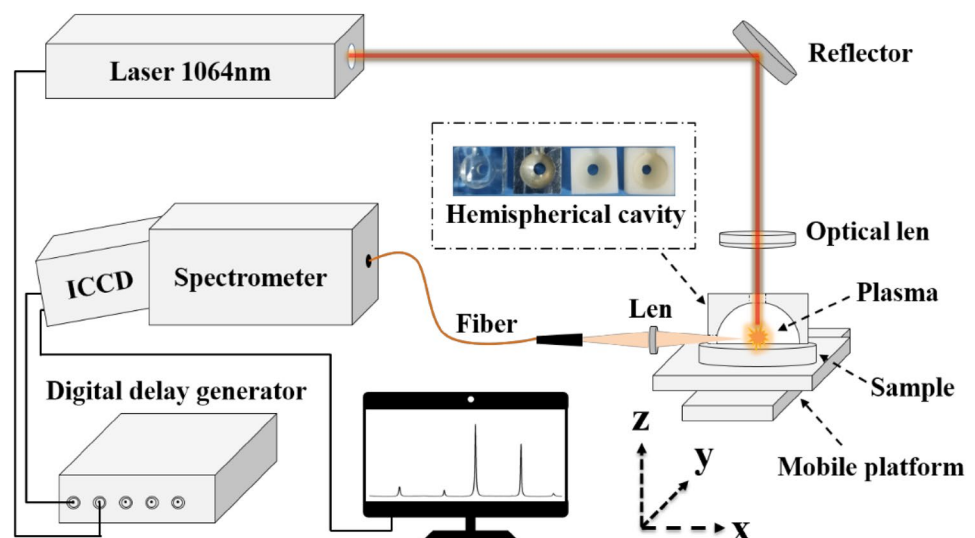
laser pulses were performed to clean the sample surface and remove surface oxides and contamination to ensure that the observed spectrum was representative of the sample composition. Samples presented for analysis were located on a fast translation stage that moved the sample between laser pulses, thereby exposing a fresh region of the sample to each successive laser pulse.

3 Results and discussion

The emission spectra of the steel alloy samples were measured both with and without confinement by the hemispherical cavity. As shown in Fig. 2, the emission spectra of the main element (Fe) and trace element (Mn) in the sample were obtained in the spectral range of 250–405 nm. It could be seen that the emission intensities for the atomic lines (Fe I: 374.55 nm, Mn I: 403.07 nm) and ionic lines (Fe II: 275.57 nm, Mn II: 259.37 nm) were all clearly enhanced.
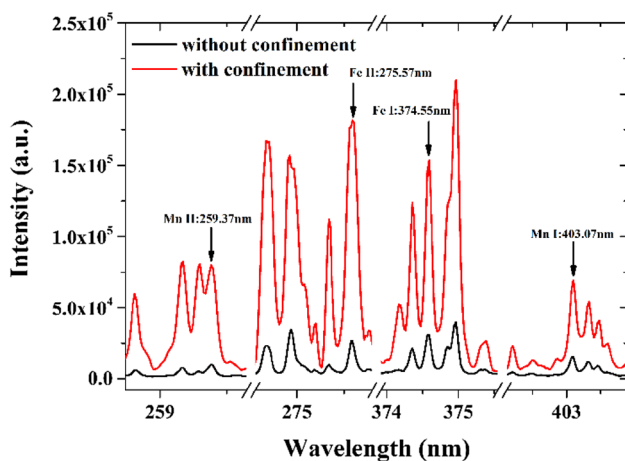

Fig. 2 Emission spectra of the steel alloy obtained both with and without hemispherical cavity

It has previously been demonstrated that the degree of spectral enhancement was related to the acquisition delay [23]. To observe the enhancement effects on the plasma clearly, a hemispherical cavity constructed of K-resin was employed to confine the plasma, while photos of the plasma were taken by ICCD. The images were acquired from 2 to 15 μs of the delay time, with a step of 1 μs. Each image was obtained from a single laser shot and all the images presented are normalized to the maximum intensity of that image for better clarity. The images were displayed in false color. To avoid the saturation of the sensitive plane of the ICCD camera, the duration of the exposure time should be small enough. Here, a gate width of 5.5 ns was set for collecting the plasma images. In addition, before collecting the plasma image of the laser-induced titanium alloy sample, a stainless steel ruler was imaged to define the magnification of the imaging system.

The images of plasma evolution both with and without the hemispherical cavity are shown in Fig. 3a, b. As can be seen, the emission intensity of the plasma without confinement decreased with increasing time delay, while the whole plasma expanded to occupy a larger volume. Therefore, the emission from the edges of the plasma weakened with increasing time delay until the emission became undetectable by ICCD. However, the emission of the plasma confined by the cavity presented a decreasing trend initially, then increased when the delay time was in the range of 6–10 μs and finally decreased faster than the unconfined plasma with increasing time delay. The shape of the plasma shrunk and became more regular, though the emission of the plasma increased. The results suggested that the hemispherical cavity compressed the plasma leading to stronger and more uniform plasma. It was also proved that the reason for the enhancement of plasma confined by the hemispherical cavity was the compression of the reflected shockwave to the plasma. A faster decrease resulting from the intense convection of the shockwave and plasma was also observed when the delay time was more than 12 μs.

Fig. 3 Images of the evolution of plasma **a** without and **b** with the confinement of the K-resin-hemispherical cavity
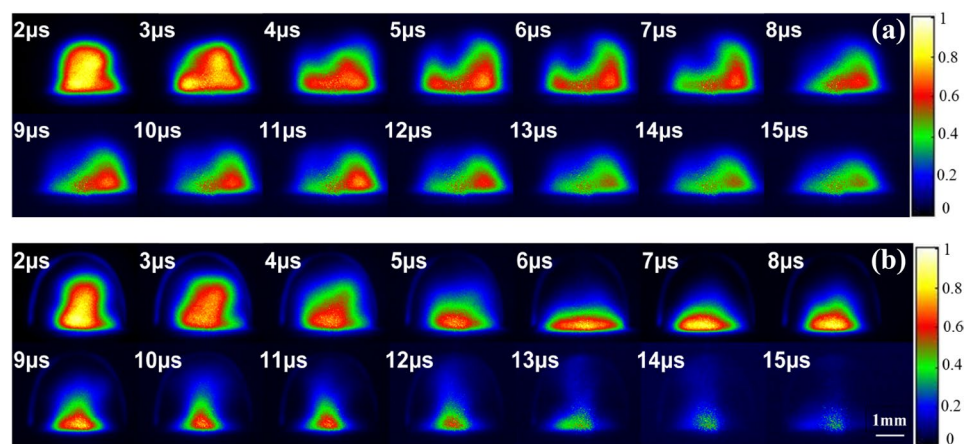
The spectral emissions were acquired with a 1 μs gate width starting from 2 up to 21 μs after the arrival of the laser pulse, with a step of 1 μs. Each spectrum was accumulated using 50 laser pulses. In the experiment, four hemispherical cavities with different materials were used to enhance the emission, including K-resin, aluminum alloy, photocurable resin, and nylon.

Figure 4 shows the temporal evolution of the enhancement factors of the atomic and ionic lines in the presence of the hemispherical cavity with different materials. Each data point represents the mean value of ten individual measurements. The error bars show the relative standard deviation for the measurements. It shows that the enhancement factors of all four lines demonstrate the same trend relative to the delay time.

When the hemispherical cavity was used, the plasma and the surrounding air were separated. In the process of plasma expansion, the interaction between the plasma and air was reduced compared to that of the unconstrained configuration. However, the enhancement of the spectral signal by the hemispherical cavity at this stage was not obvious, which can be seen in Fig. 4 that the enhancement factor was smaller (about 1–2) when the delay time changes from 2 to 6 μs. Whereas the enhancement factors increase rapidly after 6 μs and reach a maximum at around 9 μs, after which they gradually decrease. The mechanism of interaction between the shockwave and the plasma can be inferred from the trend of curve. In the first 6 μs, the plasma and the shockwave were both in the diffusion state. Since the shockwave travelled faster than the plasma, it

acted on the inner wall of the hemispherical cavity and was reflected back along its original path. When the delay time reached 6 μs, the plasma and the reflected shockwave interacted with each other. The duration of the interaction lasted about 3 μs. During this period, the plasma was compressed to the ablation point by the shockwave, resulting in the rapid increase of plasma emission. At the same time, the kinetic energy of the shockwave was completely transformed into internal energy of the plasma. Thus, when the delay time extended past 9 μs, the plasma emission decreased and finally dissipated due to the intense convection of the shockwave and the plasma. Throughout the whole process, the effect of the shockwave seemed to delay the diffusion of the plasma. In fact, the shockwave compressed the plasma into a smaller volume and did not merely restrain it, which can be seen in Fig. 3.

Figure 5 shows the best enhancement factors for the different emission lines with cavities made of four different materials. It can be seen that the enhancement effect of the same cavity material on varying atoms and ions was very different. The hemispherical cavity enhanced the ion lines, respectively. The maximum enhancement factors for Fe II:259.37 nm, Mn II:275.57 nm, Fe I: 374.55 nm and Mn I: 403.07 nm were 10.2, 11.2, 5.85 and 5.39, respectively. During the process of shockwave compression of the plasma, because of the decrease in the plasma volume, the concentration of the particles in the plasma increased. Thus, reverse bremsstrahlung, the photoionization effect, and the number of particle collisions increased, which resulted in a large number of neutral atoms ionizing into ions and free

Fig. 4 The amplification of the emission lines with confinement by hemispherical cavity in different materials, **a** Fe I: 374.55 nm, **b** Mn I: 403.07 nm, **c** Fe II: 275.57 nm, **d** Mn II: 259.37 nm
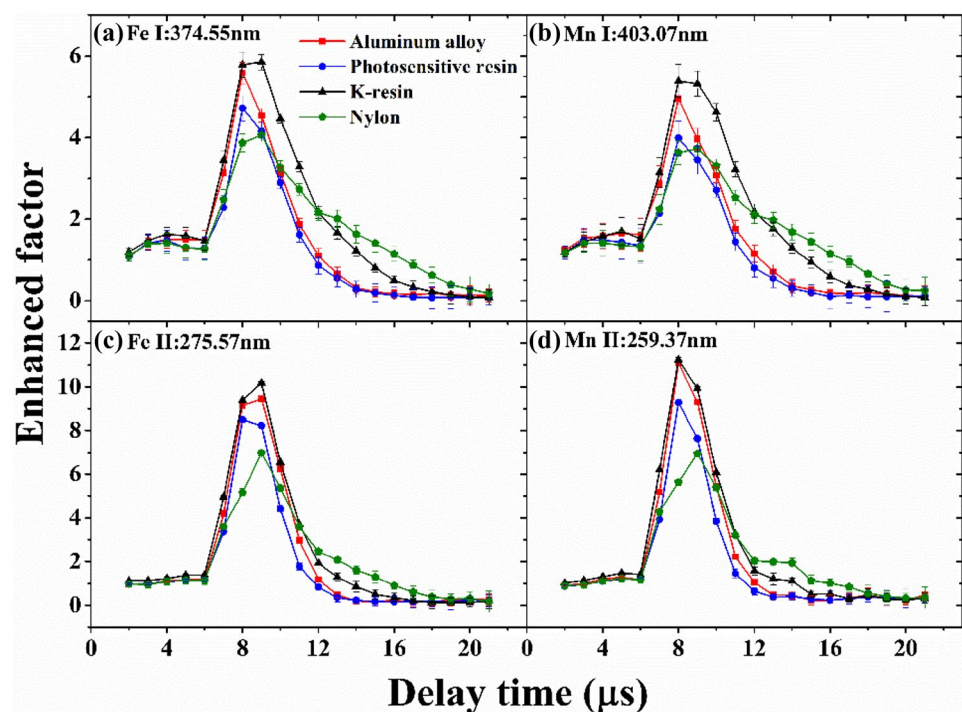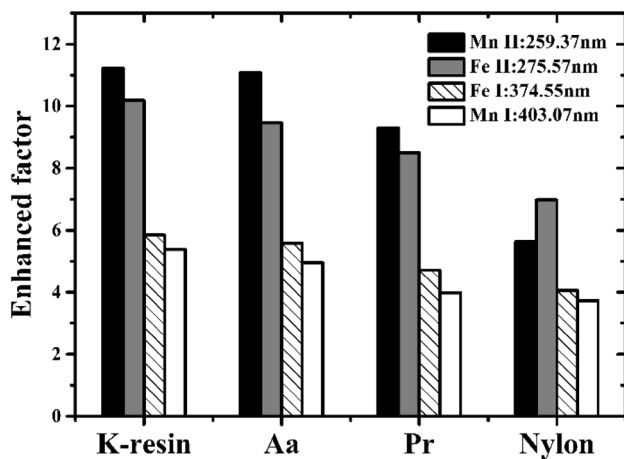
Fig. 5 The optimal amplification of the lines using hemispherical cavities of various materials

electrons. Therefore, it represented a greater enhancement of the ion lines compared to the atomic lines.

As can be seen in Fig. 5, when the enhancement factors of emission intensities with different cavities are compared, it can be seen that the different cavity materials yield different enhancement factors for the same lines. The hemispherical cavity in K resin can cause the highest enhancement factor, and the nylon hemisphere cavity has the worst enhancement effect. The reason for this phenomenon is mainly due to the difference in physical properties of the four materials.

Li et al. [16] have pointed out that the relative permittivity of the confinement rings affect the spectral signal enhancement. Their analysis indicates that when the plasma was generated, the shockwave and the electromagnetic emission from the plasma were both struck and reflected by the inner wall of the constraining unit. The enhancement effect of the spectral was not only due to the external mechanical force of the reflected shockwave to the plasma, but also due to the reflected electromagnetic wave limiting the electromagnetic field of the plasma. A material with higher relative permittivity would reflect more electromagnetic wave energy, and thus the enhancement effect was also better.

However, according to the results of the research on plasma expansion dynamics [27–29], the velocity of the shockwave and the plasma was almost the same in the early stage of expansion. Due to the counter-pressure of the ambient gas, the kinetic energy of the plasma was rapidly reduced, and expansion speed was dropped. As the delay time increased, the plasma separated from the shockwave. Then, the shockwave rapidly evolved into a hemispherical shape. The plasma reaches a maximum expansion radius diameter and gradually ceases to expand. Therefore, it has been explained by Fu et al. [15] that the main reason for the spectral enhancement was the compression of the reflected shockwave to the plasma. The shockwave was

a mechanical wave, and its reflection characteristics are not directly related to the relative permittivity. So it can be considered that the permittivity of the material hardly affects the enhancement effect.

The interaction between the shockwave and the constrained layer was always related to the rigidity and surface characteristics of the material [24–26]. The rigidity of materials can be characterized mainly by hardness. The hardness of the four hemispherical listed in our study was measured using the Shore durometer. The Shore hardness of K resin, aluminum alloy, photosensitive resin, and nylon is 87, 91, 80, 76, respectively. It can be seen that there is no significant difference in the hardness values of the four materials. It is known that the smaller the hardness of the material, the easier it is to deform. If the shockwave causes the deformation of the hemispherical cavity, the momentum of the shockwave will change during the interaction between the shockwave and the restraint layer. That is, if the cavity was deformed, the velocity of the shockwave will decrease, which will result in the change of the delay time of enhancement of the plasma emission. However, it can be seen in Fig. 4 that all the spectral signal of plasma confined by these four different hemispherical cavity began to show significant enhancement when the acquisition delay was 6 μs. This indicates that the velocity of the shockwave was almost equal under the hemispherical cavity made in different materials in our experiment, which means that all the four hemispherical cavities have not undergone significant differences of deformation during the experiment. It can be proved that the differences of the effect of the rigidity of the four materials on the reflected shockwave were negligible.

Therefore, we conclude that the main factor which influences the interaction between the shockwave and the constraint layer is the surface characteristic of the cavity. The surface characteristic is mainly reflected in the change of coating and surface roughness. There is no coating on the surface of the hemispherical cavity in our study, so we only consider the effect of the surface roughness of the material on the shockwave reflection. The surface roughness (Ra) of the four cavities was measured. It is 0.2, 0.8, 2.0, 16.1 for K resin, aluminum alloy, photosensitive resin, and nylon, respectively. According to the theory of spatial confinement, a shockwave was generated at the center of the hemispherical cavity and rapidly expanded outwards in a hemispherical shape and left the plasma eventually. After this, the shockwave directly encountered the internal wall of the hemispherical cavity and was reflected back along the original path. It is reasonable to speculate that the surface roughness of the hemispherical cavity materials had an effect on the shockwave. Shockwave is a kind of mechanical wave with the characteristics of longitudinal wave, and its reflection characteristics are similar to light waves.
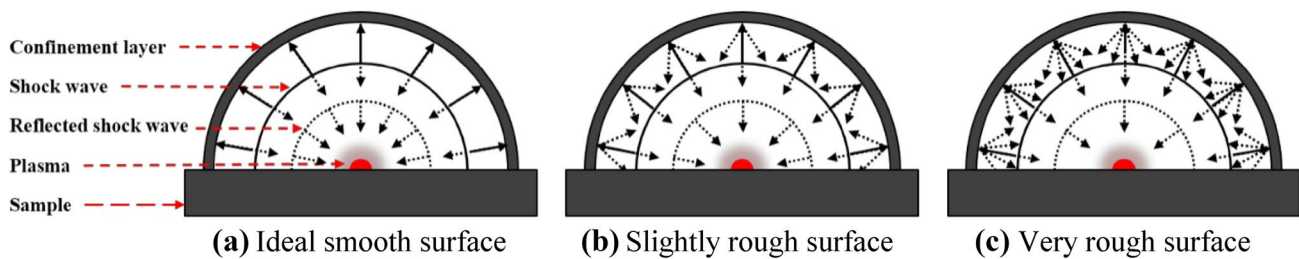
Fig. 6 Effect of surfaces of different roughness on the reflection of the shockwave. (The solid and dashed lines represent the shockwave and reflected shockwave, respectively. The solid and dashed arrows represent the direction of the shockwave and reflected shockwave, respectively)

As is commonly known, when light is incident to a surface with varying roughness, the degree of the diffuse reflection varies as a result of the varying surface reflectivity. The surface reflection characteristics for different roughness values can be described using the bidirectional reflection distribution function, which mainly consists of a specular reflection component, a direction reflection component and a uniform diffuse reflection component. The specular reflection component has the greatest effect on spectral signal enhancement. Therefore, in this study, the focus remained on the specular reflection component, which is a function of the surface roughness [30]:

$$f_r^{sp} = \frac{\rho_s}{\cos\theta_i d\Omega_i} \cdot \Delta = \frac{|F|^2 \cdot e^{-g} \cdot S}{\cos\theta_i d\Omega_i} \cdot \Delta, \qquad (1)$$

where

$$g = \frac{2\pi\sigma}{\lambda}\left(\cos\theta_r - \cos\theta_i\right). \qquad (2)$$

f_r^{sp} represents the specular reflection component. ρ_s is the specular reflectivity, Δ is a delta function, g is the surface roughness function, σ is the effective root mean square height of the rough surface, S is the shadowing function, and F is the Fresnel reflectance function.

According to Eqs. (1) and (2), the rougher the surface, the greater is the specular component. At the period of the shockwave interaction with the inner surface of the hemispherical cavity, the varying reflectivity of the surface caused a varying component of the shockwave to propagate in the direction of the specular reflection, as can be seen in Fig. 6. If the cavity had a perfectly smooth inner surface, the shockwave would be fully reflected back along its original path. The plasma would thus encounter a violent compression due to the shockwave, which would cause the best enhancement effect on the plasma emission. Material surfaces that are slightly or very rough can reflect only a certain amount of the shockwave in such a way that it will effectively interact with the plasma which thus decreases the associated enhancement effect. In summary, the degree of enhancement of the plasma emission was reduced as the surface roughness of the hemispherical cavity increased. In this experiment, the K-resin cavity with the lowest surface roughness (0.2) demonstrated the largest enhancement factor, and the nylon cavity with the highest surface roughness (16.1) exhibited the smallest enhancement factor on the plasma emission.

4 Conclusion

In this study, the plasma plume images with and without confinement were compared first. It has shown that the emission of plasma with confinement increased when the delay time was in the range of 6–10 μs and the shape of the plasma shrunk and became more regular. The results verified that the enhancement effect could be explained that the reflected shockwave compressed the plasma leading to stronger and more uniform plasma. In addition, it was observed that the enhancement effect was related to the physical properties of the cavity. Four cavities in different materials, which include K-resin, aluminum alloy, photosensitive resin and nylon, were used to confine the plasma in our study. We conclude that the main factor affecting the enhancement was the surface roughness of the cavity. The hemispherical cavity with the smallest surface roughness value (0.2) demonstrated the best enhancement effect on plasma, and the enhancement effects decreased with increasing hemispherical cavity surface roughness. A model of the effect of cavities with different surface roughness values on the reflection of the shockwave was established. These results demonstrated that it was necessary to employ a confinement layer with a low surface roughness value to enhance the plasma emission.

References

1. A.I. Chernov, M.A. Kozhaev, A. Khramova, A.N. Shaposhnikov, A.R. Prokopov, V.N. Berzhansky, Control of the phase of the

magnetization precession excited by circularly polarized femto-second-laser pulses. Photonics Res. **6**, 1079–1083 (2018)

2. L.L. Yan, Y.Y. Zhang, Z.Y. Tai, P. Zhang, X.F. Zhang, W.G. Guo, S.G. Zhang, H.F. Jiang, Multi-cavity-stabilized ultrastable laser. Chin. Opt. Lett. **16**, 121403 (2018)

3. L. Radziemski, D. Cremers, A brief history of laser-induced breakdown spectroscopy From the concept of atoms to LIBS 2012. Spectrochim. Acta Part B Atom. Spectrosc. **87**, 3–10 (2013)

4. Galbács and Gábor, A critical review of recent progress in analytical laser-induced breakdown spectroscopy. Anal. Bioanal. Chem. **407**, 7537–7562 (2015)

5. D. Girón, T. Delgado, J. Ruiz, L.M. Cabalin, J.J. Laserna, In-situ monitoring and characterization of airborne solid particles in the hostile environment of a steel industry using stand-off LIBS. Measurement **115**, 1–10 (2018)

6. U.A. Taparli, L. Jacobsen, A. Griesche, K. Michalik, D. Mory, T. Kannengiesser, In situ laser-induced breakdown spectroscopy measurements of chemical compositions in stainless steels during tungsten inert gas welding. Spectroc. Acta Part B Atom. Spectrosc. **139**, 50–56 (2018)

7. S. Moncayo, S. Manzoor, J.D. Rosales, J. Anzano, J.O. Caceres, Qualitative and quantitative analysis of milk for the detection of adulteration by Laser Induced Breakdown Spectroscopy (LIBS). Food Chem. **232**, 322–328 (2017)

8. R. Wiens, S. Maurice, J. Lasue, O. Forni, R. Anderson, S. Clegg et al., Pre-flight calibration and initial data processing for the ChemCam laser-induced breakdown spectroscopy instrument on the Mars Science Laboratory rover. Spectrochim. Acta Part B Atom. Spectrosc. **82**, 1–27 (2013)

9. D.S. Vogt, K. Rammelkamp, S. Schröder, H.W. Hübers, Molecular emission in laser-induced breakdown spectroscopy an investigation of its suitability for chlorine quantification on Mars. Icarus **302**, 470–482 (2018)

10. C. Li, X. Gao, Q. Li, C. Song, J.Q. Lin, Spectral enhancement of laser-induced breakdown spectroscopy in external magnetic field. Plasma Sci. Technol. **17**, 919–922 (2015)

11. P. Liu, D. Wu, L. Sun, R. Hai, J. Liu, H. Ding, Magnetic field selective enhancement of Li I lines comparing Li II line in laser ablated lithium plasma at 10(-2) mbar air ambient gas. Spectrochim. Acta Part B Atom. Spectrosc. **137**, 77–84 (2017)

12. P.K. Diwakar, S.S. Harilal, J.R. Freeman, A. Hassanein, Role of laser pre-pulse wavelength and inter-pulse delay on signal enhancement in collinear double-pulse laser-induced breakdown spectroscopy. Spectrochim. Acta Part B Atom. Spectrosc. **87**, 65–73 (2013)

13. E. Tognoni, G. Cristoforetti, Basic mechanisms of signal enhancement in ns double-pulse laser-induced breakdown spectroscopy in a gas environment. J. Anal. At. Spectrom. **29**, 1318–1338 (2014)

14. Z.Y. Hou, Z. Wang, J.M. Liu, W.D. Ni, Z. Li, Combination of cylindrical confinement and spark discharge for signal improvement using laser induced breakdown spectroscopy. Opt. Express **22**, 12909–12914 (2014)

15. Y.T. Fu, Z.Y. Hou, Z. Wang, Physical insights of cavity confinement enhancing effect in laser-induced breakdown spectroscopy. Opt. Express **24**, 3055–3066 (2016)

16. A. Li, S. Guo, N. Wazir, K. Chai, L. Liang, M. Zhang, Y. Hao, P.F. Nan, R.B. Liu, Accuracy enhancement of laser induced breakdown spectra using permittivity and size optimized plasma confinement rings. Opt. Express **25**, 27559–27569 (2017)

17. X. Gao, L. Liu, C. Song, J.Q. Lin, The role of spatial confinement on nanosecond YAG laser-induced Cu plasma. J. Phys. D Appl. Phys. **48**, 175205 (2015)

18. Z. Wang, Z.Y. Hou, S.L. Lui, D. Jiang, J.M. Liu, Z. Li, Utilization of moderate cylindrical confinement for precision improvement of laser-induced breakdown spectroscopy signal. Opt. Express **20**, A1011–A1018 (2012)

19. Z.Y. Hou, Z. Wang, J.M. Liu, W.D. Ni, Z. Li, Signal quality improvement using cylindrical confinement for laser induced breakdown spectroscopy. Opt. Express **21**, 15974–15979 (2013)

20. X.W. Li, Z. Wang, X.L. Mao, R.E. Russo, Spatially and temporally resolved spectral emission of laser-induced plasmas confined by cylindrical cavities. J. Anal. At. Spectrom. **29**, 2127–2135 (2014)

21. X.J. Su, W.D. Zhou, H.G. Qian, Optimization of cavity size for spatial confined laser-induced breakdown spectroscopy. Opt. Express **22**, 28437–28442 (2014)

22. L.B. Guo, Z.Q. Hao, M. Shen, W. Xiong, X.N. He, Z.Q. Xie, M. Gao, X.Y. Li, X.Y. Zeng, Y.F. Lu, Accuracy improvement of quantitative analysis by spatial confinement in laser-induced breakdown spectroscopy. Opt. Express **21**, 18188–18195 (2013)

23. X.L. Li, J.G. Wang, L.P. Zhang, X.Z. Li, Temporal and spatial evolution characteristics of plasma confined by hemispherical cavity. Acta Opt. Sin. **38**, 0830001-1–0830001-7 (2018)

24. J.Z. Zhou, J.C. Yang, M. Zhou, Y.K. Zhang, D.H. Guo, H.X. Wu, Experimental study on the effects of overlay properties on laser-induced shockwave. Chin. J. Las. **29**(11), 1041–1044 (2002)

25. X. Hong, S.B. Wang, D.H. Guo, H.G. Wu, J. Wang, Y.S. Dai, X.P. Xia, Y.N. Xie, Confining medium and absorptive overlay: their effects on a laser-induced shockwave. Opt. Laser Eng. **29**(6), 447–455 (1998)

26. P. Peyre, R. Fabbro, Laser shock processing: a review of the physics and applications. Opt. Quant. Electron. **27**(12), 1213–1229 (1995)

27. N. Arnold, J. Gruber, J. Heitz, Spherical expansion of the vapor plume into ambient gas: an analytical model. Appl. Phys. A Mater. Sci. Process. **69**(S1), S87–S93 (1999)

28. S. Harilal, B. O'Shay, Y. Tao, M.S. Tillack, Ambient gas effects on the dynamics of laser-produced tin plume expansion. J. Appl. Phys. **99**(8), 083303 (2006)

29. S. Harilal, G. Miloshevsky, P. Diwakar, N. LaHaye, A. Hassanein, Experimental and computational study of complex shockwave dynamics in laser ablation plumes in argon atmosphere. Phys. Plasmas **19**(8), 083504 (2012)

30. X.D. He, K.E. Torrance, F.X. Sillion, D.P. Greenberg, A comprehensive physical model for light reflection. Conference on Computer Graphics & Interactive Techniques. ACM. **25**(4), 175–186 (1991).